



Interfacial and emulsifying properties of amaranth (*Amaranthus hypochondriacus*) protein isolates under different conditions of pH

Jorge L. Ventureira^a, Agustín J. Bolontrade^a, Francisco Speroni^a, Elisabeth David-Briand^b, Adriana A. Scilingo^a, Marie-Hélène Ropers^b, Frank Boury^c, María C. Añón^a, Marc Anton^{b,*}

^a Centro de Investigación y Desarrollo en Criotecnología de Alimentos (CIDCA) (CONICET–CCT–La Plata – Facultad de Ciencias Exactas, UNLP), 47 y 116, La Plata (1900), Buenos Aires, Argentina

^b Institut National de la Recherche Agronomique, UR 1268 Biopolymères Interactions Assemblages, Equipe Interfaces et Systèmes Dispersés, INRA, BP 71627, F-44316 Nantes Cedex 3, France

^c L'unam, Université d'Angers, INSERM U646 "Ingénierie de la vectorisation particulière", IBS-CHU Angers, 4 rue Larrey, 49933 Angers Cedex 9, France

ARTICLE INFO

Article history:

Received 31 March 2011

Received in revised form

11 July 2011

Accepted 15 July 2011

Keywords:

Amaranth

Interfacial properties

Dilatational interfacial rheology

Langmuir isotherm

Emulsifying properties

ABSTRACT

Amaranth proteins have adequate amino acid balance for substituting either partly or completely animal proteins in human nutrition. However, they present poor emulsifying properties in basic conditions corresponding to their extraction medium. Consequently their use in acidic conditions could be envisaged to better exploit their potentialities. To better understand their emulsifying properties we have studied their interfacial activities at pHs 2.0 and 8.0 and tried to make the link between 2D and 3D properties.

Our results clearly demonstrate the better properties of AI at pH 2.0 than at pH 8 in terms of protein solubility, spreading, adsorption, viscoelastic properties of interfaces and emulsion stability. These results are in relation with the denaturated state of proteins at pH 2.0 where proteins form a harder interfacial film, as compared to pH 8.0. Thus the potential use of amaranth proteins in emulsifying applications should be oriented towards acidic applications.

© 2011 Published by Elsevier Ltd.

1. Introduction

All the prospective studies announce at the horizon 2050 a shortage of animal proteins that could induce difficulties to ensure sustenance of the entire earth population. Therefore it is necessary to target new sources of proteins with good nutrition quality. The most promising source is plant proteins that could substitute either partly or completely animal proteins in human nutrition (Rodríguez Patino et al., 2007; Tavano, Da Silva Jr., Demonte & Neves, 2008). Among the nonconventional seeds as sources of proteins, amaranth is one of the main capable, with a high protein content (14–19%) (Salcedo-Chávez, Osuna-Castro, Guevara-Lara, Domínguez-Domínguez, & Paredes-López, 2002) and an amino acid composition high in lysine and sulphur amino acids, better than those of cereals and legumes (Guzmán-Maldonado & Paredes-López, 1998; Thanapornpoonpong, Vearasilp, Pawelzik, & Gorinstein, 2008). The main fractions in amaranth isolates are albumins (10–40 kDa) and multimeric globulins with molecular weights of more than

180 kDa (Barba de la Rosa, Paredes-López, & Gueguen, 1992; Bressani & García-Vela, 1990; Martínez & Añón, 1996).

Besides their good amino acid balance, the functional properties of amaranth proteins is important for food processing, and can be modified by extraction processes (Fidantsi & Doxastakis, 2001; Tömösközi et al., 2008). The whole isolate does not exhibit good emulsifying and foaming properties at pH 8.0 (Tömösközi et al., 2008). Amaranth albumins (main fraction) have a higher emulsifying activity at pH 5.0 while amaranth globulins exhibit their higher emulsifying properties at pH 7.0 (Silva-Sanchez, Gonzales-Castenada, de Leon-Rodriguez & Barba de la Rosa, 2004). The use of the amaranth protein isolates in food is thus conditioned by pH. In order to improve the interfacial activity of amaranth protein isolates, their hydrolysates were produced (Ventureira, Martínez, & Añón, 2010). Whatever the degree of hydrolysis and the action of enzyme (alcalase or trypsin) the increase in emulsifying activity is not strong enough to retain this pathway.

Consequently, acidification seems to be a good track as the emulsifying properties of the isolates are higher at pH 2.0 than at pH 8.0 (Ventureira et al., 2010) and this was attributed to the lower size of polypeptides and a better solubility of proteins at pH 2.0.

* Corresponding author.

E-mail address: marc.anton@nantes.inra.fr (M. Anton).

However, this latter paper did not advance any explanation on the behavior of amaranth proteins at the interfaces in relation with the understanding of their emulsifying properties at pH 2.0 and 8.0.

Consequently, to better understand the potential of amaranth proteins as food emulsifiers, we have investigated their structure by circular dichroism and differential scanning calorimetry, and their interfacial activity at both air–water and oil–water interfaces at pH 2.0 and pH 8.0, and tried to connect these data to the stability of emulsions. Additionally we have compared the emulsifying properties of total protein fraction and only soluble fraction in view to assess the impact of aggregates.

2. Materials and methods

2.1. Amaranth seeds and flour

The seeds of amaranth were obtained from the Universidad Nacional de La Pampa (Argentina). They were ground in an Udy mill (UDY Corp. Fort Collins, CO) 1 mm mesh and screened by 10 xx mesh (Universidad Nacional de La Plata, Argentina), to obtain the flour. It was defatted by extraction with hexane (10% w v⁻¹ suspension) during 24 h at room temperature, under continuous stirring during the first 5 h. Protein content of flour was 23.1 ± 0.2% (w w⁻¹), obtained by Kjeldahl method (AOAC, 1984) using a protein/N factor of 5.85 (Scilingo, Molina Ortiz, Martínez, & Añón, 2002).

2.2. Preparation of protein isolate (AI)

The amaranth protein isolate was prepared according to Martínez and Añón (1996). The previously defatted flour was suspended in water in a relation 1:10 and the pH of the suspension was adjusted to 9.0 by the addition of 2 mol L⁻¹ NaOH solution. The suspension was stirred during 1 h and then centrifuged at 9000 g for 20 min at 10 °C. The pH of the supernatant was adjusted to 5.0 with 2 mol L⁻¹ HCl and centrifuged at 4 °C for 20 min at 9000 g. The precipitate was suspended in water, neutralized with 0.1 mol L⁻¹ NaOH and freeze-dried. The protein content of isolate was 80.6 ± 1.0% (dry basis) as determined by Kjeldahl method.

2.3. Protein suspension

Suspensions of amaranth protein isolate (AI) were prepared in buffers at pH 2.0 (0.052 mol L⁻¹ H₃PO₄, 0.048 mol L⁻¹ Na₃PO₄, 0.050 mol L⁻¹ NaCl, ionic strength 0.1) and pH 8.0 (0.0025 mol L⁻¹ NaH₂PO₄, 0.0325 mol L⁻¹ Na₂HPO₄, ionic strength 0.1). Reagents were from Sigma Chemicals (St. Louis, MO) with analytical grade. Buffer solutions were prepared with ultra pure water (MilliQ).

2.4. Soluble fraction of amaranth isolate

Amaranth isolate was suspended in the buffers at pH 2.0 and 8.0 at a protein concentration of 1 g L⁻¹ then stirred for 1 h at room temperature and centrifuged at 10000 g for 30 min at 20 °C. The protein content of the supernatant was determined using the Lowry method modified by Markwell (Markwell, Haas, Bieber, & Tolbert, 1978). The solubility is given by the ratio between the protein contents in the supernatant and the total protein content. In these conditions, the protein solubility of AI suspensions was 91.1 ± 3.4% at pH 2.0 and 74.9 ± 5.6% at pH 8.0. The higher solubility rate in comparison to a previous publication results from the higher ionic strength used in this study (Ventureira et al., 2010).

2.5. Differential scanning calorimetry (DSC)

DSC measurements were performed in a TA Q100 (TA-Instruments, New Castle, DE) calorimeter calibrated at a heating rate of 10 °C min⁻¹ with indium, lauric acid, and stearic acid. Hermetically sealed aluminium pans were prepared to contain 10–15 mg of isolate suspended in the buffers at pH 2.0 and 8.0 (10% w v⁻¹); a double empty pan was employed as reference. Capsules were heated from 20 to 140 °C at a rate of 10 °C min⁻¹. After each run pans were punctured and their dry-matter content was determined by leaving the pans overnight in an oven at 105 °C and weighted. The denaturation temperature (Td) and enthalpy of transition (ΔH) were obtained by analyzing the thermograms with the Software Universal Analysis 2000 (version 4.4A. Software Plus V5.41).

2.6. Circular dichroism (CD)

Secondary structure differences in soluble protein solutions from AI at pH 2.0 and 8.0 were determined by the absorbance of polarized light in the 190–250 nm UV range. Samples were suspended 1 h at room temperature in a quantity to have a soluble protein concentration of 1 g L⁻¹. They were centrifuged at 10000 g for 30 min at 20 °C then the supernatant was poured in a quartz measure cell with a light path of 0.1 mm length. CD measurements were carried out in a spectropolarimeter Jobin-Yvon CD6 (Jobin-Yvon SA, Longjumeaux, France). Molar ellipticity, θ (deg × cm² dmol⁻¹) was calculated as Jiang, Chen, and Xiong (2009) assuming an average molecular weight of the amino acids in AI of 130. Samples were analyzed by duplicate and five spectra of each sample were used.

2.7. Zeta-potential measurements

The zeta-potential values of AI suspended in water at different pH values: 2.0, 4.0, 6.0 and 8.0, were measured by a laser Doppler velocimetry and phase analysis light scattering technique using a Malvern Zetasizer Nano ZS instrument (Malvern Instruments Ltd., Worcestershire, UK) at 20 °C. One mL of diluted sample (approximately 0.5 g L⁻¹) was put in the electrophoresis cell.

2.8. Langmuir isotherms

The soluble fraction of AI was spread at the air–liquid interface on fully automated Wilhelmy balance Nima 601 BAM (Nima Technologies, Coventry, England) containing the buffer. The balance is equipped with a Wilhelmy plate sensor connected to a force transducer that measures continuously the surface pressure (π). The surface pressure is defined as the difference between the surface tension of the buffer and that due to the protein film. The soluble fraction was prepared from a 2 g L⁻¹ suspension of AI. The quantity of proteins spread at the surface was 35 μg contained in 100 μL of buffer. Portions of 5 μL of protein solution were deposited carefully with a syringe in 20 different points distributed all along the surface at 20 °C. The protein was allowed to adsorb and stabilize at the surface for 1 h at 20 °C. The surface pressure-area isotherm determination was performed at 20 ± 0.2 °C with a rate of 40 cm² min⁻¹.

2.9. Interfacial tension and rheological properties of the oil-water interface

The dynamic interfacial tension (γ) measurements between oil and water were made using an automated drop tensiometer (Tracker IT-Concept, Longessaigne, France), described by Benjamins, Cagna, and Lucassen-Reynders (1996), with a rising drop of oil in the

aqueous media. The apparatus analyzes the variation of the drop axial symmetric shape that was digitized and analyzed through a CCD camera coupled to a video image profile digitizer that processed the drop profiles according to the Laplace equation using Windrop software (I.T.-Concept, France).

An Exmire microsyringe (ITO Corporation, Tokyo, Japan) with an U-shaped needle containing the oil is immersed in a cuvette with the protein solution. The axisymmetric drop is formed to reach a volume of 8 μL that means approximately an interfacial area of 18 mm^2 .

The aqueous media contained the soluble fraction of AI in different concentrations (0.05–1 g L^{-1}) in the buffers described above. The temperature was controlled by a circulated bath at 20 $^{\circ}\text{C} \pm 0.1$ $^{\circ}\text{C}$. The measurements were performed during 15000 s. Commercial sunflower oil from Lesieur (France) was passed by a silica column WAT051900 (Waters, Milford, MA) before use to extract polar molecules like phospholipids, free fatty acids and lipolysis or oxidation products.

The same tensiometer was used to make the measurements of the interfacial dilatational rheology. Periodical sinusoidal compressions and expansions of the drop volume were made. The surface dilatational modulus (E) was determined by the variation of the interfacial tension ($d\gamma$) resulted from a small change of the relative interfacial area (dA/A_0) in the linear region of viscoelasticity. E was defined as (Gibbs, 1928): $E = d\gamma (dA/A_0)^{-1}$.

The frequencies of the oscillations varied from 0.005 to 0.05 Hz after 15000 s (equilibrium state) to check the response of the rheological parameters at different rates of oscillations.

Alternatively, at a concentration of 0.1 g L^{-1} the oscillations were made at 0.02 Hz in a wide range of times to observe the relationships between the interfacial tension and the dilatational modulus. The rheological parameters, elastic and viscous dilatational modulus, were taken from the variation and time of response of the interfacial tension with the oscillations. The area variations of the droplet surface were $\pm 5\%$ of the initial interfacial value, which has been determined to enter in the linear region of viscoelasticity.

2.10. Preparation of oil-water emulsions

Emulsions were prepared with either the total protein or the soluble fraction of AI. In both cases, the concentration of the protein sample was 5 g L^{-1} in the aqueous phase. Emulsions were prepared homogenizing 550 μL of sunflower oil (Lesieur, France) and 5 mL of the protein sample with an ultra sound homogenizer Sonics Vibracell 500W (Sonic & Materials INC., Newtown, CT) at a power level of 3.5, in pulsation mode (50%) during 5 min, using the tapered tip immersed 15 mm in the liquid of the mixture contained in a plastic tube. The tube was placed into an ice bath to reduce heating during homogenization.

2.11. Droplet size distribution

The particle size distribution of the emulsions was determined using a Saturn Digsizer 5200 (Micromeritics Instrument Corporation, Norcross, GA) laser light scattering instrument immediately after emulsion preparation. In order to measure the individual droplet size, 125 μL of the emulsions were poured in a tube containing 2875 μL of 1% SDS solution to avoid flocculation. The measurement consists in recirculating diluted emulsions until an obscuration level of 8–13% is measured. Volume (%) diameter distributions were obtained. Mean Sauter diameters, $d_{3,2}$, were calculated as: $d_{3,2} = \sum_{i=1}^N (n_i \times d_i^3) / \sum_{i=1}^N (n_i \times d_i^2)$.

The variation in values of $d_{3,2}$ at different times, in the presence or absence of SDS, was used to calculate a flocculation index (F) and a coalescence index (C):

$$F = (d_{3,2 t} - d_{3,2 t + \text{SDS}}) / d_{3,2 t + \text{SDS}}$$

$$C = (d_{3,2 t + \text{SDS}} - d_{3,2 \text{ in} + \text{SDS}}) / d_{3,2 \text{ in} + \text{SDS}}$$

where $d_{3,2 t}$ is the value of $d_{3,2}$ at any time, $d_{3,2 t + \text{SDS}}$ is $d_{3,2}$ measured in the presence of SDS and $d_{3,2 \text{ in} + \text{SDS}}$ is the initial value of $d_{3,2}$ measured in the presence of SDS. The measurements were made 1 day or 7 days after emulsion preparation (storage at room temperature).

2.12. Statistical analysis

Data were averaged from at least two independent assays. Results are reported as mean \pm standard deviation. Statistical analysis was carried out by the OriginPro 8 software (OriginLab Co., Northampton, MA). Analyses of variance were conducted. Differences between the sample means were analyzed by Fisher-LSD test using $\alpha = 0.05$.

3. Results

3.1. Differences of structure of AI proteins at pH 2.0 and 8.0

The suspensions of AI at pH 2.0 and pH 8.0 were analyzed by DSC (Fig. 1). At pH 2.0 no significant endothermic peak was observed while two endothermic peaks with denaturation temperatures (T_{d1} and T_{d2}) of 70.2 $^{\circ}\text{C}$ and 98.8 $^{\circ}\text{C}$ and enthalpy values of 2.2 and 8.3 J g^{-1} were detected at pH 8.0. The T_d values are similar to those previously obtained by Martínez and Añón (1996) and Avanza and Añón (2007).

The disappearance of the denaturation peaks at pH 2.0 suggests that the acidic pH induces an extensive unfolding of amaranth proteins and that practically no native structure persists in the proteins. On the contrary, the proteins keep their compact ordered globular conformation at pH 8.0. Similarly, different authors have reported a dissociation and unfolding of the tertiary and quaternary structures of the oligomers of soybean glycinin at acidic pH (Puppo & Añón, 1999).

The far UV CD spectra of the soluble fractions of AI at pH 2.0 and pH 8.0 are shown in Fig. 2. At pH 8.0, a maximum in molar ellipticity is observed at 193 nm. This peak was attributed to the presence of

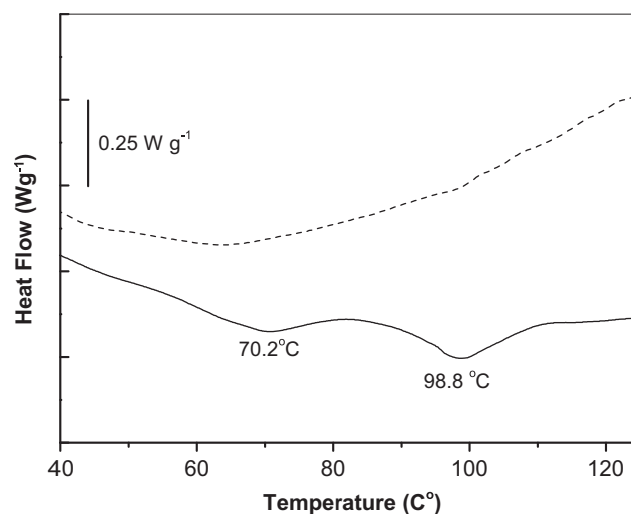


Fig. 1. DSC thermograms of AI suspensions (10% w v^{-1}) at pH 2.0 (—) and 8.0 (---). The temperatures of thermal denaturation are indicated below the peaks. The rate of run was 10 $^{\circ}\text{C min}^{-1}$.

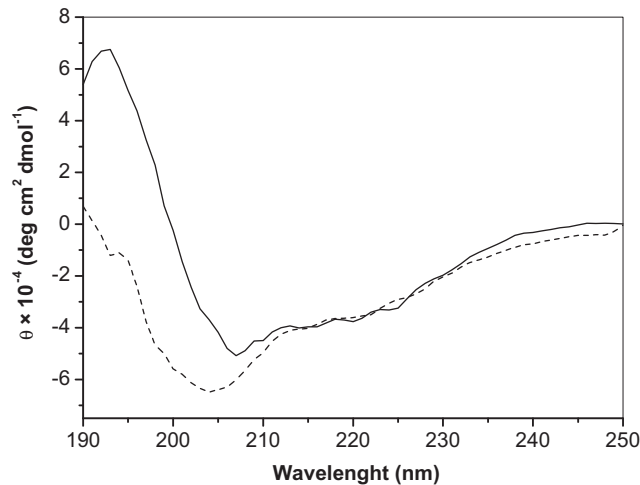


Fig. 2. Far-UV circular dichroism spectra for AI proteins (1 g L^{-1}) at pH 2.0 (--) and 8.0 (–) in the 190–250 UV range. Samples were analyzed in duplicate.

secondary structures such as α -helix or β -sheet (Chen, Yang, & Chau, 1974). At pH 2.0, this maximum could not be distinguished, suggesting that these structures are more abundant at pH 8.0 than at pH 2.0. At pH 8.0, the minimum was observed at 207 nm while it was shifted to lower wavelengths (204 nm) at pH 2.0. As the random coil arrangement shows minimum values around 195 nm (Chen et al., 1974), the shift detected from 207 to 204 nm suggests a higher quantity of random coil at pH 2.0. β -turns present a maximum at 207 nm (Greenfield, 1996) while the α -helix structure shows minimum values at 207 and 222 nm. The smaller ellipticity values observed at 207 nm at pH 2.0 than at pH 8.0 as well as the same ellipticity values over 212 nm indicate a smaller quantity of β -turns in the global conformation at pH 2.0. Consequently, the far UV CD spectra suggest that the soluble protein fraction of AI contains less structured domains at pH 2.0 than at pH 8.0.

Zeta potential values of AI suspensions at different pHs showed that the average electric charge of the mixture of proteins was positive at pH 2.0 (25 mV) and negative at 8.0 (–30 mV). These results are in agreement with the mean isoelectric point reported between 4.5 and 6.5 for different amaranth protein fractions by Konishi, Horikawa, Oku, Azumaya, and Nakatani (1991).

3.2. Interfacial behavior

3.2.1. Air–water interfaces

Comparing the behaviors at pH 2.0 and pH 8.0, it can be observed that the highest values of surface pressure (π) were reached by proteins at pH 2.0 all along the curve (Fig. 3 a). For the same area/protein ratio π was more elevated at pH 2.0 than at pH 8.0. This suggests that proteins are more easily spread at the interface at pH 2.0 than pH 8.0. The curves of the first derivative from the Langmuir isotherms (Fig. 3 b) show clearly two inflexion points at pH 8 at values of 0.18 and 0.33 $\text{m}^2 \text{mg}^{-1}$. These inflexion points reflect the change in organization of the biopolymers at the air–water interface versus pressure. The lack of inflexion points at pH 2.0 indicates that in this condition proteins are in a more advanced denaturation state inducing a reduced subsequent reorganization inside the interfacial film.

3.2.2. Oil–water interfaces

The kinetics of adsorption at the oil–water interface at both pH and several concentrations of the soluble protein fraction are

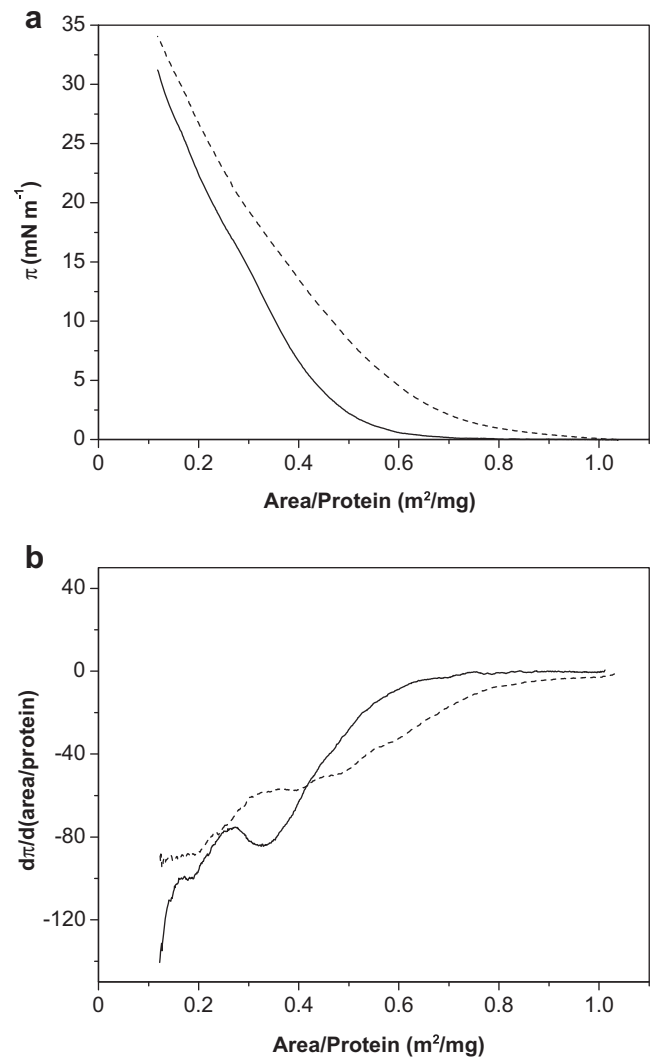


Fig. 3. (a) Surface pressure isotherms of AI proteins ($35 \mu\text{g}$ in $100 \mu\text{L}$ buffer) at pH 2.0 (--) and 8.0 (–). (b) First derivative from the surface pressure isotherms at pH 2.0 (--) and 8.0 (–).

shown in Fig. 4 a and b. At any concentration, the interfacial tension (γ) at a fixed time is smaller at pH 2.0 than at pH 8.0. After 15000 s in a 1 mg mL^{-1} concentrated solution, γ reached a final value of around 8 mN m^{-1} at pH 2.0 m^{-1} while γ decreased down to 11 mN m^{-1} at pH 8.0. This indicates a slightly better capability to adsorb at the interface and undergo rearrangements of proteins at pH 2.0 than at pH 8.0.

Fig. 5 a shows the rise of the complex dilatational modulus versus the time of adsorption. Whatever the pH, this modulus is clearly supported by its elastic component (E') whereas the viscous one (E'') did not influence it strongly (results not shown). For this reason, we have expressed only the complex dilatational modulus.

These results highlight the higher values of the modulus obtained at pH 2.0 from the beginning of the experiment. At the end it was about 3 times higher at the acidic pH than at basic pH. It is noteworthy that at pH 2.0, at 0.05 h of adsorption (first point) the value of dilatational modulus was similar to those reached by the proteins at pH 8.0 at the end of the experience. Fig. 5 b plots the dilatational modulus versus the interfacial tension for both pH values. While the dilatational modulus at pH 2.0 reached 30 mN m^{-1} at a surface tension of 20 mN m^{-1} , the same value was achieved at 12.5 mN m^{-1} at pH 8.0. These results show that the

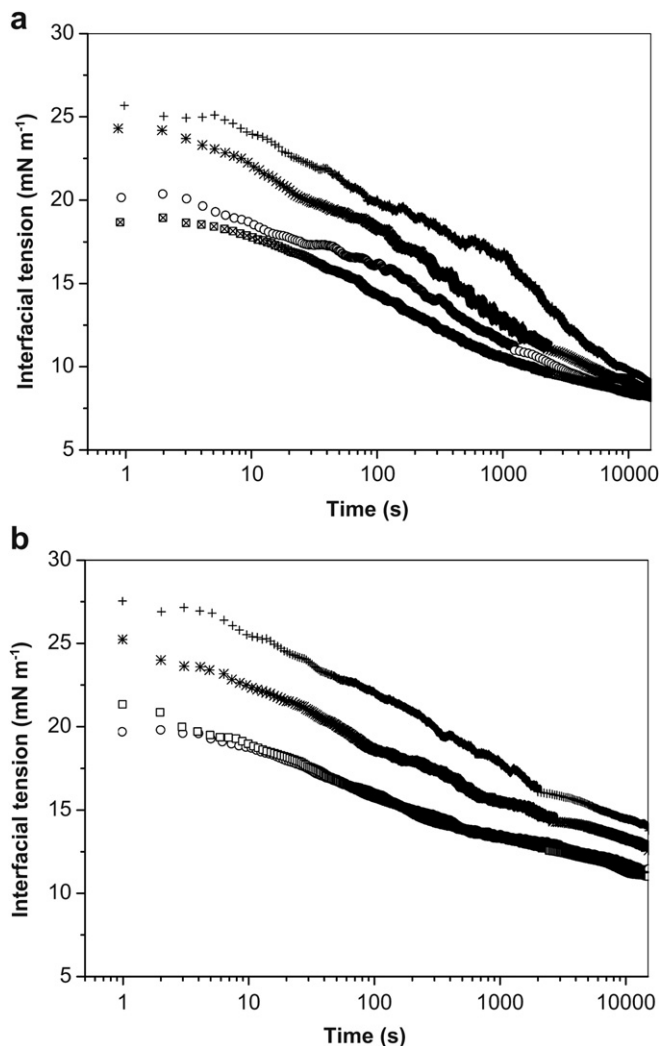


Fig. 4. Dynamic interfacial tension of AI proteins at the oil-water interface at pH 2.0 (a), and pH 8.0 (b) versus the concentrations in the aqueous phase: +: 0.05 g L⁻¹; *: 0.1 g L⁻¹; ○ 0.5 g L⁻¹; ◻ 1 g L⁻¹.

interface at pH 2.0 is much more elastic and potentially less susceptible to rupture. Moreover, the slopes obtained from these plots are different between pH 2.0 and 8.0, confirming differences in the structural characteristics of protein films.

3.3. Emulsions

Droplet size distribution of emulsions made with the soluble fraction or the total protein fraction of AI at pH 2.0 and 8.0 are shown in Fig. 6. It can be seen that the emulsions made at pH 2.0 were very stable against coalescence with practically no appearance of droplets with higher diameters during storage, for both the soluble and the total protein fractions (Fig. 6 a and b). At the same pH, flocculation occurred in the emulsions, more strongly in those prepared with the total protein fraction than in those made with only the soluble protein fraction.

At pH 8.0 (Fig. 6 a), droplets exhibited a slightly weaker stability against coalescence evidenced by the increase of population of droplets with diameters of about 10 μm during the storage. At pH 8.0, flocculation was observed with both soluble and total protein fractions, especially in the emulsions made with the total protein (Fig. 6 c and d). Table 1 lists the values of d_{3,2} as well as the

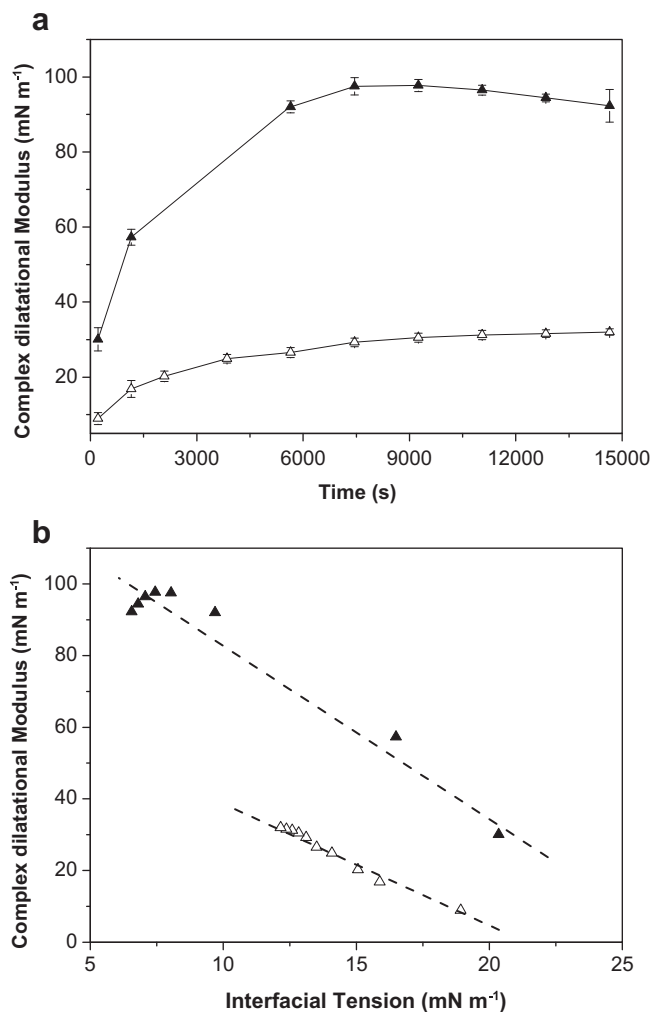


Fig. 5. (a) Variation of the complex dilatational modulus of AI protein interfaces with the time of adsorption at pH 2.0 (▲) and 8.0 (△) at a concentration of 0.1 g L⁻¹ and 0.02 Hz. (b) Variation of the complex dilatational modulus of AI protein interfaces with the variation of the interfacial tension at pH 2.0 (▲) and 8.0 (△) at a concentration of 0.1 g L⁻¹ and 0.02 Hz.

flocculation and coalescence indexes (F and C respectively) for all emulsions at different storage times. It formalizes the information described from the droplet size distributions: i) the coalescence occurred only in the emulsions made at pH 8.0, ii) the flocculation was more important in the emulsions made with the total protein fraction at both pH values.

4. Discussion

4.1. How to explain the difference of interfacial properties between the two pHs?

At pH 8.0, DSC and CD showed that the proteins contain structures such as helices and β-turns (CD) that are denatured around 80 °C (DSC). The proteins keep most probably its globular native structure at pH 8.0. Usually, the compact globular structure diminishes the possibilities of the polypeptides to rearrange and to reorient at the interface. Additionally, the presence of β-turns was related with the loss of surface activity because of the decrease of molecular flexibility (Razumovsky & Damodaran, 1999).

At pH 2.0, the proteins present in the soluble and total protein fractions of AI were denatured (as demonstrated by DSC and CD)

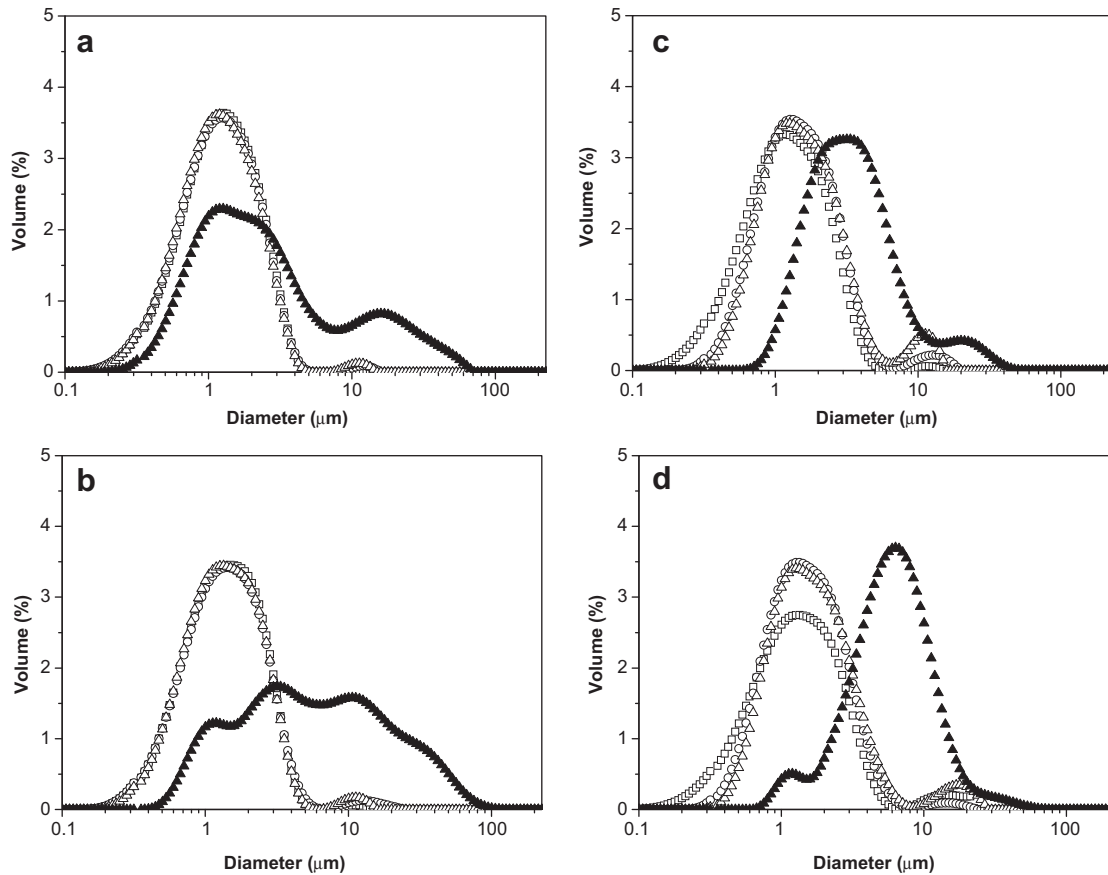


Fig. 6. Size distribution of emulsions prepared with AI (5 g proteins L⁻¹) at different times expressed in volume (%) in the following conditions (a) pH 2.0 soluble protein; (b) pH 2.0 total protein; (c) pH 8.0 soluble protein; (d) pH 8.0 total protein. The different distributions in each graphic are: □ : initial emulsion in presence of SDS, ○ : initial emulsion without SDS, △ : 7 days stored emulsion in presence of SDS and ▲ : 7 days stored emulsion without SDS.

without influence on their solubility (approx. 91% solubility). This may explain the better efficiency of proteins to cover the interface. First, the loss in β -turns may enhance the interfacial activity (Razumovsky & Damodaran, 1999). Second, disordered, small and flexible proteins reduce the surface tension earlier and faster than ordered, rigid and larger proteins (Beverung, Radke, & Blanch, 1999). Unfolded proteins have more freedom to take geometrical dispositions that favor the decrease in interfacial energy and to

reduce the surface tension. For the same reason, the structure of the proteins at pH 2.0 is less compact than at pH 8.0 and a smaller amount of protein is needed to cover the same area. Consequently the thickness of the interface is expected to be thinner at pH 2.0 than at pH 8.0. This assertion was verified by measuring the non adsorbed protein amount in the emulsions formulated with the proteins suspended at pH 2.0 and at pH 8.0. At pH 2.0 the quantity of non adsorbed proteins present in the aqueous phase of the emulsions was two times higher than at pH 8.0 (results not shown). In conclusion, the denaturation induced by pH leads to a better interfacial activity. It can be noticed that a similar behavior has been observed with lysozyme (Xu & Damodaran, 1993).

Table 1

Volume (%) diameter ($d_{3,2}$), flocculation index (F) and coalescence index (C) of emulsions prepared with AI (5 g proteins L⁻¹) at pH 2.0 and 8.0 with soluble and total protein, measured at different times.

Parameter	Time of storage			
	pH/Fraction	Initial	1 day	7 days
$d_{3,2}$ (SDS)	pH 2.0 _{tot}	0.85 ± 0.06 _{a b}	0.85 ± 0.09 _{a b}	0.87 ± 0.07 _{a b}
	pH 2.0 _{sol}	0.73 ± 0.10 _a	0.74 ± 0.11 _a	0.75 ± 0.09 _a
	pH 8.0 _{tot}	0.71 ± 0.04 _a	0.96 ± 0.04 _{b c}	1.02 ± 0.03 _c
	pH 8.0 _{sol}	0.72 ± 0.06 _a	0.96 ± 0.02 _{b c}	1.01 ± 0.05 _c
F	pH 2.0 _{tot}	4.3 ± 0.3 _{a b}	8.4 ± 1.3 _{c d}	9.7 ± 0.8 _{c d}
	pH 2.0 _{sol}	3.5 ± 1.7 _{a b}	4.0 ± 3.3 _{a b}	4.7 ± 1.9 _{a b c}
	pH 8.0 _{tot}	10.7 ± 2.0 _{c d}	13.2 ± 0.0 _d	21.3 ± 0.2 _e
	pH 8.0 _{sol}	5.9 ± 3.9 _{b c}	3.8 ± 4.5 _{a b}	3.3 ± 4.3 _a
C	pH 2.0 _{tot}	—	0.0 ± 0.0 _a	0.3 ± 0.1 _a
	pH 2.0 _{sol}	—	0.1 ± 0.1 _a	0.2 ± 0.1 _a
	pH 8.0 _{tot}	—	3.5 ± 0.2 _b	4.3 ± 0.5 _b
	pH 8.0 _{sol}	—	3.4 ± 0.9 _b	4.1 ± 0.6 _b

Values with similar identical letters for each property indicates that the means difference is not significant at the 0.05 level (Fisher LSD 95%).

4.2. Are we able to relate interfacial characteristics and emulsifying properties ?

The rheological measurements of the interfaces showed higher values of dilatational modulus in the case of pH 2.0 as compared to pH 8.0. It is known that surface elasticity is much lower for flexible proteins than for globular ones (Lucassen-Reynders, Fainerman, & Miller, 2004). In our case we hypothesise that at pH 2.0 amaranth proteins are in a more denatured state whereas at pH 8.0 the globular structure is more preserved. This behavior should lead to a higher surface elasticity at pH 8.0 but we observed the opposite result. It appears then that interactions between adsorbed proteins inside the interfacial film could play a major role in the film reinforcement through hydrophobic, hydrogen or electrostatic interactions. As zeta potentials were clearly high whatever the pH

(25 mV at pH 2.0 and –30 mV at pH 8.0) the track leading to hydrogen or hydrophobic interactions has to be followed to better explain these results.

Finally, the differences in elasticity at the interface can be linked to the resistance of emulsions against coalescence (Izmailova, Yampolskaya, & Tulovskaya, 1999; Langevin, 2000). More precisely, we can consider that, as the principle of the method consists in sinusoidal deformations of the oil drop area, it can be put in relation with the phenomena occurring during storage or transport of emulsions. If we take this into account, emulsions at pH 2.0 should be more stable against coalescence than those at pH 8.0 and this was confirmed in our results.

Additionally, the fact that the emulsions made with total proteins showed more flocculation than those made with soluble protein originated from the nature of the sample used for the homogenization. The non soluble proteins could be adsorbed in two different interfaces at the same time and have been produced bridging flocculation. Furthermore, such aggregates may also induce depletion flocculation if they are sufficiently small. We will have to explore these hypotheses for a future study.

5. Conclusion

Our results clearly show that the potential use of amaranth proteins in emulsifying applications would be oriented at acidic pH instead of basic pH. This conclusion is based on the better properties of AI at pH 2.0: (1) protein solubility, (2) spreading (a-w interfaces), (3) adsorption (o-w interfaces), (4) viscoelastic properties (o-w interfaces), and (5) emulsion stability.

Acknowledgments

This work was supported by the Ecos-Sud Project of France and SECyT of Argentina (N° A07B05).

References

- AOAC. (1984). In *Official methods of analysis* (14th ed). Arlington, VA, USA: Association of Official Analytical Chemists.
- Avanza, M. V., & Añón, M. C. (2007). Effect of thermal treatment on the proteins of amaranth isolates. *Journal of the Science of Food and Agriculture*, 87(4), 616–623.
- Barba de la Rosa, A. P., Paredes-López, O., & Gueguen, J. (1992). Characterization of amaranth globulins by ultracentrifugation and chromatographic techniques. *Journal of Agricultural and Food Chemistry*, 40(6), 937–940.
- Benjamins, J., Cagna, A., & Lucassen-Reynders, E. H. (1996). Viscoelastic properties of triacylglycerol/water interfaces covered by proteins. *Colloids and Surfaces A: Physicochemical and Engineering Aspects*, 114, 245–254.
- Beverung, C. J., Radke, C. J., & Blanch, H. W. (1999). Protein adsorption at the oil/water interface: characterization of adsorption kinetics by dynamic interfacial tension measurements. *Biophysical Chemistry*, 81(1), 59–80.
- Bressani, R., & García-Vela, L. A. (1990). Protein fractions in amaranth grain and their chemical characterization. *Journal of Agricultural and Food Chemistry*, 38(5), 1205–1209.
- Chen, Y. H., Yang, J. T., & Chau, K. H. (1974). Determination of the helix and β^2 form of proteins in aqueous solution by circular dichroism. *Biochemistry*, 13(16), 3350–3359.
- Fidantsi, A., & Doxastakis, G. (2001). Emulsifying and foaming properties of amaranth seed protein isolates. *Colloids and Surfaces B: Biointerfaces*, 21(1–3), 119–124.
- Gibbs, J. W. (1928). *Collected works*. New York: Longmans.
- Greenfield, N. J. (1996). Methods to estimate the conformation of proteins and polypeptides from circular dichroism data. *Analytical Biochemistry*, 235(1), 1–10.
- Guzmán-Maldonado, S. H., & Paredes-López, O. (1998). Production of high-protein flours as milk substitutes. In J. R. Whitaker, F. Shahidi, A. López-Munguia, R. Y. Yada, & G. Fuller (Eds.), *Functional properties of proteins and lipids*, vol. 708 (pp. 66–79). Washington D. C.: American Chemical Society.
- Izmailova, V. N., Yampolskaya, G. P., & Tulovskaya, Z. D. (1999). Development of the Rehinder's concept on structure-mechanical barrier in stability of dispersions stabilized with proteins. *Colloids and Surfaces A: Physicochemical and Engineering Aspects*, 160(2), 89–106.
- Jiang, J., Chen, J., & Xiong, Y. L. (2009). Structural and emulsifying properties of soy protein isolate subjected to acid and alkaline pH-shifting processes. *Journal of Agricultural and Food Chemistry*, 57(16), 7576–7583.
- Konishi, Y., Horikawa, K., Oku, J., Azumaya, J., & Nakatani, N. (1991). Extraction of two albumin fractions from amaranth grains: comparison of some physicochemical properties and the putative localization in the grains. *Agricultural and Biological Chemistry*, 55(11), 2745–2750.
- Langevin, D. (2000). Influence of interfacial rheology on foam and emulsion properties. *Advances in Colloid and Interface Science*, 88(1–2), 209–222.
- Lucassen-Reynders, E. H., Fainerman, V. B., & Miller, R. (2004). Surface dilatational modulus or Gibbs' elasticity of protein adsorption layers. *Journal of Physical Chemistry B*, 108, 9173–9176.
- Markwell, M. A. K., Haas, S. M., Bieber, L. L., & Tolbert, N. E. (1978). A modification of the Lowry procedure to simplify protein determination in membrane and lipoprotein samples. *Analytical Biochemistry*, 87(1), 206–210.
- Martínez, E. N., & Añón, M. C. (1996). Composition and structural characterization of Amaranth protein isolates. An electrophoretic and calorimetric study. *Journal of Agricultural and Food Chemistry*, 44(9), 2523–2530.
- Puppo, M. C., & Añón, M. C. (1999). Soybean protein dispersions at acid pH. Thermal and rheological properties. *Journal of Food Science*, 64(1), 50–56.
- Razumovsky, L., & Damodaran, S. (1999). Surface Activity-compressibility relationship of proteins at the air-water interface. *Langmuir*, 15(4), 1392–1399.
- Rodríguez Patino, J. M., Miñones Conde, J., Linares, H. M., Pedroche Jiménez, J. J., Carrera Sánchez, C., Pizones, V., et al. (2007). Interfacial and foaming properties of enzyme-induced hydrolysis of sunflower protein isolate. *Food Hydrocolloids*, 21(5–6), 782–793.
- Salcedo-Chávez, B., Osuna-Castro, J. A., Guevara-Lara, F., Domínguez-Domínguez, J., & Paredes-López, O. (2002). Optimization of the isoelectric precipitation method to obtain protein isolates from amaranth (*Amaranthus cruentus*) seeds. *Journal of Agricultural and Food Chemistry*, 50(22), 6515–6520.
- Scilingo, A. A., Molina Ortiz, S. E., Martínez, E. N., & Añón, M. C. (2002). Amaranth protein isolates modified by hydrolytic and thermal treatments. Relationship between structure and solubility. *Food Research International*, 35(9), 855–862.
- Silva-Sanchez, C., Gonzalez-Castaneda, J., de Leon-Rodriguez, A., & Barba de la Rosa, A. P. (2004). Functional and rheological properties of amaranth albumins extracted from two Mexican varieties. *Plant Foods for Human Nutrition*, 59, 169–174.
- Tömösközi, S., Gyenge, L., Pelcéder, A., Varga, J., Abonyi, T., & Lásztity, R. (2008). Functional properties of protein preparations from amaranth seeds in model system. *European Food Research and Technology*, 226(6), 1343–1348.
- Tavano, O. L., Da Silva, S. I., Jr., Demonte, A., & Neves, V. A. (2008). Nutritional responses of rats to diets based on chickpea (*Cicer arietinum* L.) seed meal or its protein fractions. *Journal of Agricultural and Food Chemistry*, 56(22), 11006–11010.
- Thanapornpoonpong, S. N., Vearasilp, S., Pawelzik, E., & Gorinstein, S. (2008). Influence of various nitrogen applications on protein and amino acid profiles of amaranth and quinoa. *Journal of Agricultural and Food Chemistry*, 56(23), 11464–11470.
- Ventureira, J., Martínez, E. N., & Añón, M. C. (2010). Stability of oil: Water emulsions of amaranth proteins. Effect of hydrolysis and pH. *Food Hydrocolloids*, 24(6/7), 551–559.
- Xu, S., & Damodaran, S. (1993). Comparative adsorption of native and denatured egg-white, human, and T4 phage lysozymes at the air-water interface. *Journal of Colloid and Interface Science*, 159(1), 124–133.